The resistance of a plate moving through mud experiments and simulations

Lovato, S.L.; Kirichek, Alex ; Toxopeus, S; Settels, Just W. ; Talmon, A.M.; Keetels, G.H.

The resistance of a plate moving through mud: experiments and simulations

Conference Paper · October 2021

CITATIONS
0

READS
5

6 authors, including:

Stefano Lovato
Delft University of Technology
3 PUBLICATIONS **0** CITATIONS
SEE PROFILE

Alex Kirichek
Delft University of Technology
45 PUBLICATIONS **135** CITATIONS
SEE PROFILE

The resistance of a plate moving through mud: experiments and simulations

Stefano Lovato[1], **Alex Kirichek**[1], **Serge Toxopeus**[2], **Just Settels**[2], **Arno Talmon**[1,3], **Geert Keetels**[1]
[1]Delft University of Technology, Delft/Netherlands.
[2] Maritime Research Institute Netherlands, Wageningen/Netherlands.
[3]Deltares, Delft/Netherlands
s.l.lovato@tudelft.nl

1 Introduction

Safe navigation in restricted areas is ensured, among others, by setting a minimum under keel clearance (UKC), which is the distance between the ship's keel and the bottom. However, in many ports and waterways around the world the seabed is covered by mud (Fig. 1) and the position of the bottom is not longer clearly defined. In this case, the depth is determined based on the *nautical bottom*, defined as "the level where physical characteristics of the bottom reach a critical limit beyond which contact with a ship's keel causes either damage or unacceptable effects on controllability and manoeuvrability"(PIANC).

A complete implementation of the nautical bottom concept therefore requires a good understanding of the possible effects of muddy bottoms on the navigation of marine vessels. Although some model-scale (Delefortrie et al. (2005)) and full-scale (Barth et al. (2016)) trials have been carried out in the past decades, results are difficult to generalise because of the large number of parameters involved (UKC, mud layer thickness, rheological properties, ship's geometry and speed, fairway cross-section, etc). Thus, for practical reasons, port authorities define the nautical bottom as the level where the mud reaches either a critical density (e.g. 1200 kg/m^3) or a critical rheological property, based on the experience acquired over the years. These criteria, however, may be too conservative in some cases, which either lead to unnecessary maintenance and environmental costs, or to excessive restrictions on the allowed draughts of the vessels.

Fig. 1: A ship moving through a muddy seabed (snapshot from www.youtube.com/watch?v=LSbQhUJMBJw).

A research project was thus started with the aim to build a Computational Fluid Dynamic (CFD) framework that would allow more systematic studies on this topic (Lovato et al. (2021)). One of the main difficulties of the CFD approach, however, is that mud exhibits a very complex non-Newtonian rheology (see e.g Shakeel et al. (2021)). Nevertheless, for engineering purposes, mud is often modelled as a Bingham fluid as it is the simplest rheological model capable of capturing one of the main features of mud, i.e. viscoplasticity. These type of fluids start to flow only when the level of shear stress exceeds a certain threshold, called yield stress. Below the yield stress, viscoplastic fluids behave as solid-like materials. Other examples of these fluids are gels, drilling fluids, cosmetic and food products (e.g mayonnaise).

The main goal of this research is to establish whether, in spite of its simplicity, the Bingham model is suitable for prediction of the forces acting on marine vessels moving through mud. Since experimental data for such scenarios are rather difficult to obtain, a simpler problem is considered here. In this paper, an experimental and numerical study on the resistance of a thin plate moving through homogeneous mud in laminar regime will be presented.

2 Experimental methods

2.1 Facility and setup

The experimental data were obtained in the "water-soil flume" (Fig. 2 (a)) at the research institute Deltares. The flume, which is 30 m long, 2.5 m high and 2.4 m wide, was filled with natural mud previ-

ously dredged from the seabed in the port of Rotterdam.

The experiments consisted in towing a smooth plywood plate through mud and measuring the total resistance. The towing speed of the carriage was varied between 0.25 and 1.0 m s^{-1} and, for each speed, the tests were repeated 8 times. The plate has been reinforced with vertical and horizontal wooden beams to increase its stiffness and to reduce possible bending. The main information about the experiments are summarised in Table 1.

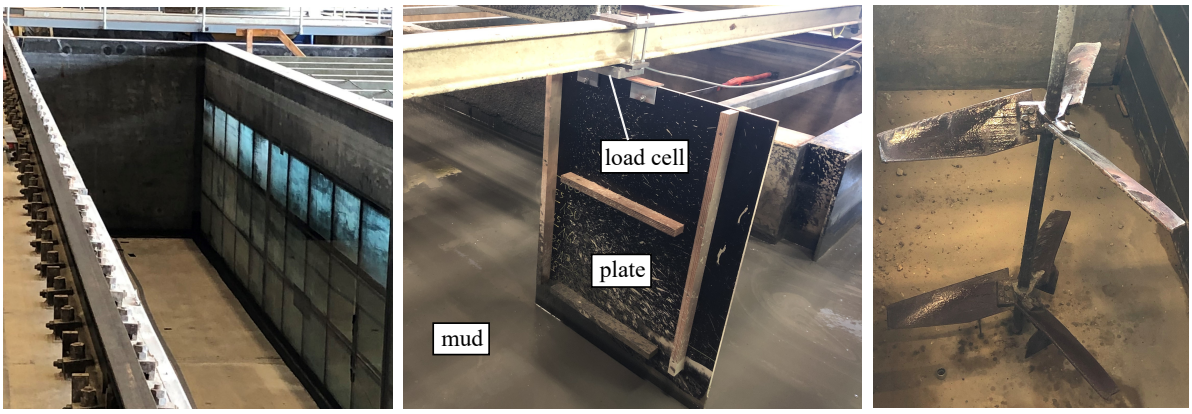

(a) (b) (c)

Fig. 2: (a) Water-soil flume at Deltares, Netherlands. (b) Plywood plate immersed in mud. (c) Mixer used to homogenise the mud in the flume.

2.2 Uncertainties

The uncertainties due to the calibration of the load cell was estimated by pulling the plate with a thread attached to a dynamometer previously calibrated using weights. The force was increased from 4 to 24 N by constant increments of 2 N. The maximum observed discrepancy between the load cell and the dynamometer was about 3.5%. It was thus decided to adopt U_{cal} = 4%, as a 'Type B' uncertainty. Another source of uncertainty originates from the scatter of the mean force obtained from the stationary part of the load cell signal. Thus, each test was repeated 8 times and the uncertainties due to the repeated tests, U_{rep}, was estimated by statistical methods, similarly to the procedure proposed by the ITTC. Assuming that the mean force follows the Student's t-distribution, k = 2.306 was adopted as coverage factor, which ensures a 95% confidence level with the 8 repetitions (degrees of freedom). The uncertainty due to the experimental setup was not estimated as the time required would have been incompatible with the time available to complete the experiments. The final experimental uncertainties U_{exp} in the mean force is thus obtained from the RMS of U_{cal} and U_{rep}, and it is within 5.1% of the experimental data for all cases.

Table 1: Main information about the experiments. Note that the mud level is 1.96 m for the thickest mud and 2.0 m otherwise.

Plate		Flume	
Chord (m)	0.8	Length (m)	30.0
Thickness (m)	0.012	Width (m)	2.4
Submerged span (m)	0.96 or 1.0	Mud level (m)	1.96 or 2.0
Speed (m/s)	0.27, 0.52, 0.77, 1.02	Height (m)	2.5

2.3 Mud preparation

The mud was collected from the Calandkanaal (port of Rotterdam) and it was transported to the water-soil flume. In order to analyse the effect of different mud rheologies, the mud was diluted with sea water (having same salinity as the natural system) to obtain three densities that correspond to target yield stress values of approximately 30, 20 and 10 Pa. To ensure the homogeneous properties within the water-soil flume, the mud was stirred using a rotating mixer (Fig. 2 (c)) that was towed three times back-and-forth prior the experiments with each mud. After the homogenisation, six samples of each mud were collected.

2.4 Mud rheology

The HAAKE MARS I rheometer was used to perform the rheological experiments on the mud samples using concentric cylinder geometry and keeping the temperature at 20 °C. The flow curves of the mud samples were obtained in controlled shear rate mode with the following protocol: (i) shear rate ramp-up from 0 to 300 s^{-1} in 180 s, (ii) constant shear rate of 300 s^{-1} for 60 s, and (iii) shear rate ramp-down from 300 to 0 s^{-1} in 180 s. This type of test is quite fast and repeatable to obtain the yield stress of remoulded samples (Shakeel et al. (2021)). The ramp-down curve for shear rates above 200 s^{-1} was then used for the least-squares fitting of the Bingham model (Fig. 3), which, for simple shear flow, reads:

$$\begin{cases} \tau = \tau_B + \mu_B \dot{\gamma} & \text{for} \quad \tau_B \leq \tau\,, \\ \dot{\gamma} = 0 & \text{for} \quad \tau < \tau_B\,, \end{cases} \tag{1}$$

where τ (Pa) is the shear stress, $\dot{\gamma}$ (s^{-1}) is the shear rate τ_B (Pa) is the yield stress and μ_B (Pa s) is the Bingham (or plastic) viscosity. The density and the Bingham parameters that were obtained from the mud samples and used in the CFD computations are reported in Table 2.

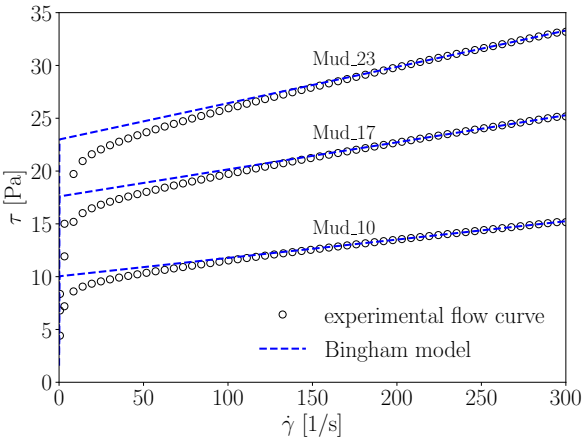

Fig. 3: Mud flow curves and Bingham fit for one of the six samples of each mud.

Table 2: Mean values of density and Bingham parameters over the six sample for each mud.

Mud case	ρ (kg/m^3)	τ_B (Pa)	μ_B (Pa s)
Mud_10	1171	9.96	0.0172
Mud_17	1190	17.3	0.0249
Mud_23	1200	23.0	0.0344

3 Numerical methods

3.1 Governing equations

Preliminary calculations have shown that the effect of the free surface with no angles of attack is within the numerical uncertainties. Therefore, double-body calculations were performed by solving the incompressible continuity and momentum equations combined with the Bingham constitute equation. However, in order to avoid numerical difficulties caused by the infinite viscosity when $\dot{\gamma} = 0$ in Eq. (1), the regularisation approach of Papanastasiou (1987) was used. The non-differentiable constitutive equation Eq. (1) was thus replaced by

$$\tau = \tau_B(1 - e^{-m\dot{\gamma}}) + \mu_B \dot{\gamma} \tag{2}$$

where m is the regularisation parameter. In the limit of $m \to \infty$, Eq. (2) tends to Eq. (1), therefore large values of m are required in order to mimic the behaviour of the ideal (non-regularised) Bingham model (Eq. (1)). For this work, m was chosen such that $m\tau_B/\mu_B = 12000$, which represents the ratio of the possible maximum and minimum viscosity attainable by the fluid.

3.2 Grids and boundary conditions

The computational domain was discretised with a series of multi-block structured H-type grids, with 1.77 million cells in the finest grid. The size of the first cell away from the plate surface is 2×10^{-4} m. For the boundary conditions, the inflow velocity was applied at the inlet boundary, whereas the no-slip/no-penetration condition was applied to the plate surface. At the outlet, Dirichlet condition was imposed for the pressure, and symmetry conditions were applied to the top and symmetry planes. Preliminary calculations showed that the presence of the plate is not 'felt' by the side and bottom walls, thus symmetry conditions were applied also to these boundaries (Fig. 4).

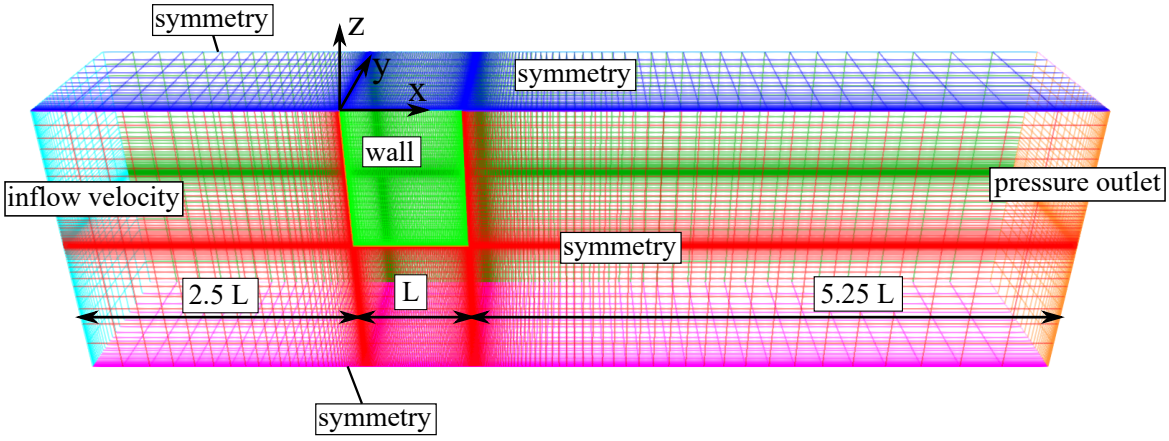

Fig. 4: Computational domain and boundary conditions.

3.3 Flow solver

The CFD code used for the present work is ReFRESCO (Vaz et al. (2009)), a viscous-flow code currently being developed and verified for maritime purposes by the Maritime Research Institute Netherlands (MARIN) in collaboration with several non-profit organisations around the world. Originally developed for Newtonian fluids, ReFRESCO has been recently extended and verified (Lovato et al. (2021)) to include the Herschel-Bulkley model, of which Bingham is just a particular case. Equations are discretised in strong-conservation form with a second-order finite-volume method for unstructured meshes with cell-centred co-located variables. Mass conservation is ensured with a pressure-correction equation based on a SIMPLE-like algorithm. The convective fluxes of the transport equations are linearised with the Picard method and discretised with the Harmonic scheme (Van Leer (1979)).

4 Validation procedure

According to the validation procedure proposed by ASME (2009), the modelling errors, δ_{model}, can be estimated by comparing two quantities: the (expanded) validation uncertainty,

$$U_{val} = \sqrt{U_{num}^2 + U_{exp}^2 + U_{input}^2} \tag{3}$$

and the comparison error, $E = S - D$, where S is the simulation value and D is the experimental value, U_{num} and U_{exp} are the numerical and experimental uncertainty, respectively, and U_{input} is the uncertainty in the simulation input parameters. E and U_{val} define an interval within which δ_{model} falls, i.e. $E - U_{val} \leq \delta_{model} \leq E + U_{val}$.

5 Input parameter uncertainties

Numerical simulations require input parameters that are experimentally determined and that have uncertainties associated with them. The input parameter uncertainties, U_{input}, were estimated using the perturbation method and by approximating the numerical data with analytical formulas for the friction and pressure components (not discussed here). For the present work, the input parameters are the: plate's draught H, carriage's speed V (inflow velocity), mud density ρ, Bingham yield stress τ_B and viscosity μ_B. For all the cases, the estimated input parameter uncertainties combined are within 2.8% of the CFD results.

6 Solution verification

Solution verification was carried out to estimate the numerical errors and uncertainties. For steady flows, numerical errors are usually divided in round-off, iterative and discretisation errors. Round-off errors arise from the finite precision of computers and, for this work, they can be neglected by using double-precision machines. Iterative errors stem from the use of iterative methods to find the solution of the discretised equations. For this work, iterations were stopped when the L_∞ norm of the normalised residuals dropped below 10^{-7}. However, this convergence tolerance was actually hardly met, thus, in practice,

calculations were stopped when the maximum number iterations was reached. As a result, iterative errors could not be neglected and the uncertainties, U_{it}, were estimated using the method proposed in Eça and Hoekstra (2009), whereas the discretisation uncertainties, U_d, were estimated with the method described in Eça and Hoekstra (2014). The total numerical uncertainty, U_{num}, was finally obtained by arithmetic summation of U_{it} and U_d. Overall, the numerical uncertainties do not exceed 2.4%.

The use of regularisation methods produces an additional error, the regularisation error, which is the difference between the solution of the regularised and the ideal (non-regularised) model. In absence of validated methods to estimate the regularisation uncertainty, U_{reg}, from numerical data, we have estimated U_{reg} adopting the same method used for U_d by replacing the grid size with $1/m$. Overall, the estimated regularisation uncertainties do not exceed 3.9%. Since the regularisation parameter affects both discretisation and iterative errors, U_{reg} was arithmetically (no RMS) added to U_{num}.

7 Results and discussion

The estimated comparison errors and the validation uncertainties are reported in Table 3 together with the upper bounds of the modelling errors, whereas the total resistance is plotted in Fig. 5 against the inflow velocity. Table 3 shows that the comparison error is often close or within the validation uncertainties, except at the lowest speed, where the comparison errors always exceed the uncertainties. In any case, E is never sufficiently larger than U_{val} to allow a direct estimate of the modelling errors and, for all the cases, only the upper bound of the modelling error could be estimated. For a few cases, also the sign of the modelling error could be determined.

Table 3: Comparison error, validation uncertainty and the upper bounds of the modelling errors in percentage of CFD data.

V (m/s)	E	U_{val}	$\lvert\delta_{model}\rvert \leq$	E	U_{val}	$\lvert\delta_{model}\rvert \leq$	E	U_{val}	$\lvert\delta_{model}\rvert \leq$
		Mud_10			Mud_17			Mud_23	
0.27	10.1	6.3	16.4 (+)	9.8	6.4	16.2 (+)	8.7	7.7	16.4 (+)
0.52	5.4	6.0	11.3	4.7	6.6	11.3	3.4	7.1	10.4
0.77	0.1	6.7	6.7	0.6	5.9	5.9	-1.0	6.1	7.2
1.02	-5.5	6.4	12.0	-7.7	6.9	14.6 (-)	-5.5	6.3	11.7

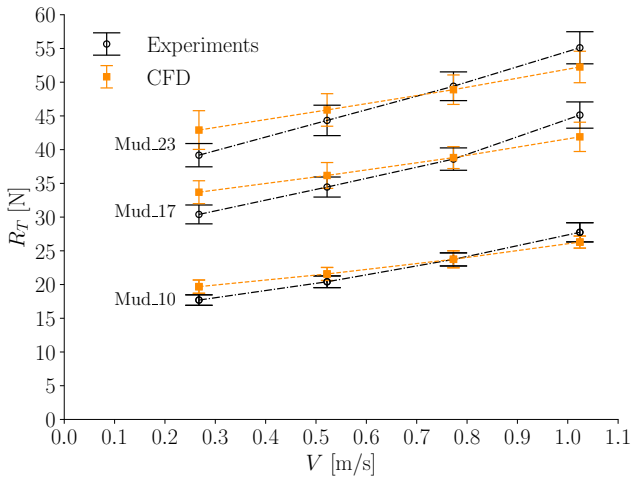

Fig. 5: Total resistance of the plate moving through mud against the inflow velocity (or towing speed).

The larger comparison errors are found at $V = 0.27$ m s^{-1}, and the upper bound of the modelling errors is about 16%. The lowest upper bound of the modelling errors is found for $V = 0.77$ m s^{-1} because of the very small comparison error for all the three mud concentrations. At this speed, there seems to be an intersection of the numerical and experimental data (see also Fig. 5). In fact, numerical data tends to overpredict the resistance at low speed and to underpredict at high speed. Figure 5 suggests that E will increase in magnitude for increasing speed, meaning that the trend in the experiments in not correctly captured by CFD. In any case, validation is achieved for nearly all the cases (i.e. for the cases where experimental and CFD uncertainties overlap) at the level of about 7% of the CFD data. If more information about the modelling error is required, the uncertainty (especially the experimental) needs to be reduced.

Further preliminary calculations (not reported here) were carried out with the aim to reduce the comparison error and better capture the trend of the experimental data. Better agreement with experimental data was achieved when calculations were performed with (i) a small rotation (about 1.5°) of the plate around the vertical axis; (ii) the effect of the free surface; (iii) lower regularisation parameters that were determined directly from the mud flow curves to better capture the behaviour at low shear rates. This suggests that the experiments, especially at the high speed, could have been contaminated by small rota-

tions of the plate, and that rheology of mud is better captured by the regularised Bingham model rather than the ideal Bingham.

8 Conclusions

The purpose of this study was to assess the performance of the Bingham model for numerical predictions of flow of mud over a plate. This was done by comparing numerical predictions with the measured resistance of a plate moving through the mud collected from the seabed in the port of Rotterdam.

Comparison with numerical data showed a fairly good agreement, with maximum discrepancies of about 10%. Since the validation uncertainty is around 6-7%, only the lower and upper bounds of the modelling errors could be estimated. The maximum upper bounds of the modelling errors are about 16% and they are found at the lowest speed considered in this study. In particular, CFD seems to overpredict the resistance at low speed, whereas underprediction is observed at high speed. However, preliminary calculations revealed that experimental data may have been contaminated by small rotations of the plate, which enhanced the free surface deformation, especially at the highest speed. These preliminary calculations also showed that the Bingham model appears to overpredict the experimental data, whereas using lower regularisation parameters might significantly improve the prediction at all speeds. In any case, results showed that, in spite of the discrepancies between experiments and CFD, the changes in the forces due to variation of the mud properties is consistent with the experiments.

In conclusion, a first step has been made to establish that the regularised Bingham model may be a good compromise between accuracy and simplicity for predicting the forces due to the laminar flow of mud over slender bodies. Future work is needed to investigate whether these conclusions are valid also for applications concerning the navigation of ships in presence of muddy seabeds, which involve turbulent flows of a water-mud system over more complex geometries.

Acknowledgement

This work is supported by the Dutch Research Council (NWO), Port of Rotterdam (PoR) and MARIN. Calculations were performed on the Marclus4 cluster (MARIN). The experimental work was carried out within the Prisma project and is funded by PoR, TU Delft, Port of Hamburg and Topconsortium voor Kennis en Innovatie (TKI) Deltatechnologie subsidy. Special thanks to Pavan Goda, Marcel Busink and Lynyrd de Wit for their contribution to the experimental part. This study was carried out within the framework of the MUDNET academic network: https://www.tudelft.nl/mudnet/.

References

ASME PTC Committee (2009). Standard for Verification and Validation in Computational Fluid Dynamics and Heat Transfer: ASME V&V 20. The American Society of Mechanical Engineers (ASME).

Barth, R., Van der Made, C.J.A.W., Bourgonjen, L., Van Dijken, J., Vantorre, M. and Verwilligen, J. (2016). Manoeuvring with negative underkeel clearance: 2nd full scale field test in the port of Delfzijl. 4th MASHCON-International Conference (pp. 262-271).

Delefortrie, G., Vantorre, M. and Eloot, K. (2005). Modelling navigation in muddy areas through captive model tests. Journal of marine science and technology, 10(4), pp.188-202. doi:10.1007/s00773-005-0210-5

Eça, L. and Hoekstra, M. (2009). Evaluation of numerical error estimation based on grid refinement studies with the method of the manufactured solutions. Computers and Fluids, 38(8), 1580–1591. doi:10.1016/j.compfluid.2009.01.003

Eça, L. and Hoekstra, M. (2014). A procedure for the estimation of the numerical uncertainty of CFD calculations based on grid refinement studies. Journal of Computational Physics, 262, 104–130. doi:10.1016/j.jcp.2014.01.006

Harbour approach channels design guidelines (2014), PIANC Report No. 121. PIANC.

van Leer, B. (1979). Towards the ultimate conservative difference scheme. V. A second-order sequel to Godunov's method. Journal of Computational Physics, 32(1), 101–136. doi:10.1016/0021-9991(79)90145-1

Lovato, S., Toxopeus, S. L., Settels, J. W., Keetels, G. H., and Vaz, G. (2021). Code Verification of Non-Newtonian Fluid Solvers for Single- and Two-Phase Laminar Flows. Journal of Verification, Validation and Uncertainty Quantification. 6(2), 021002. doi:10.1115/1.4050131.

Papanastasiou, T.C. (1987). Flows of materials with yield. Journal of Rheology, 31(5), pp.385-404. doi:10.1122/1.549926

Shakeel, A., Kirichek, A., Talmon, A. and Chassagne, C. (2021). Rheological analysis and rheological modelling of mud sediments: What is the best protocol for maintenance of ports and waterways? Estuarine, Coastal and Shelf Science, 257, 107407. doi:10.1016/j.ecss.2021.107407

Vaz, G., Jaouen, F. and Hoekstra, M. (2009). Free-Surface Viscous Flow Computations: Validation of URANS Code FRESCO. Proceedings of OMAE2009, Honolulu, Hawaii, USA, 425–437. doi:10.1115/OMAE2009-79398